Materials Science and Engineering A 549 (2012) 228–232

Contents lists available at SciVerse ScienceDirect

Materials Science and Engineering A

journal homepage: www.elsevier.com/locate/msea

Compressive failure of Al alloy matrix syntactic foams manufactured by melt infiltration

X.F. Tao [1], Y.Y. Zhao *

School of Engineering, University of Liverpool, Liverpool L69 3GH, UK

ARTICLE INFO

Article history:
Received 4 April 2012
Received in revised form 11 April 2012
Accepted 16 April 2012
Available online 22 April 2012

Keywords:
Syntactic foam
Liquid metal infiltration
Mechanical characterisation
Failure
Fracture

ABSTRACT

Al alloy syntactic foams containing hollow or porous ceramic microspheres were fabricated by melt infiltration. Tensile, shear, confined compressive and unconfined compressive tests were performed and the failure modes in compression were studied. The tensile and shear strengths were insensitive to the types of the ceramic microspheres. In confined compression, all syntactic foams failed by progressive collapse of the microspheres. Different failure mechanisms were observed in unconfined compression. The syntactic foams with stronger ceramic microspheres failed by Griffith rupture, with cracks oriented at approximately 30° to the loading direction and the compressive strengths being about eight times of their tensile strengths. The syntactic foams with weaker ceramic microspheres failed by progressive collapse of the ceramic microspheres and had lower compressive strengths.

1. Introduction

Metal matrix syntactic foams are composite materials consisting of a continuous metal matrix embedded with hollow or porous ceramic particles [1–20]. They have higher strengths than polymeric syntactic foams and can be used as lightweight structures at higher temperatures and in more harsh environments. They are also capable of absorbing impact energies, because the porosity inside the materials can provide extensive strain accumulation. Compared with metal foams with the same alloy matrix, they are usually cheaper to produce and have higher yield strengths. They have great potential for applications as energy absorbers where a high plateau stress is desirable, for example, automobile bumpers.

Metal matrix syntactic foams have certain structural characteristics similar either to polymeric syntactic foams or to metal foams. The characteristics of compressive deformation of polymeric syntactic foams and metal foams, however, are very different. Metal foams are normally ductile in compression. The plastic deformation is typified by gradual collapse and crushing of the foam cells, maintaining a relatively low plateau stress until the onset of densification [21]. In contrast, polymeric syntactic foams often fail in a brittle manner under compression. The mode of failure can be longitudinal split, shear fracture, wedge shaped cracking or a combination of these modes [22–24].

Different compressive deformation behaviours and failure mechanisms have been observed in metal matrix syntactic foams. Both ductile failure, due to the crushing of the embedded ceramic particles and the subsequent collapse of the metal network [5,8,11–13], and brittle fracture [4,5,8,11,12] are common. However, the conditions that favour one failure mode or other are not well understood. Furthermore, the brittle fracture failure was often attributed to shear failure. In some cases, however, the orientations of the cracks with respect to the loading direction deviated significantly from 45° [12]. This indicates that the fracture mechanisms in metal matrix syntactic foams are more complicated than those in metallic materials.

In this study, Al alloy syntactic foams with an Al 6082 alloy matrix containing different types of hollow and porous ceramic microspheres were fabricated by pressure melt infiltration. Tensile, shear, confined compressive and unconfined compressive tests were performed. The compressive failure modes were studied and discussed.

2. Experimental

The raw materials used for fabricating the Al alloy syntactic foam samples were Al 6082 alloy and a ceramic microsphere powder. The powder was supplied by Pty Ltd Australia and has a composition of ~60% SiO_2, ~40% Al_2O_3 and 0.4–0.5% Fe_2O_3 by weight. The microspheres of the powder have two different kinds of inner structure, either hollow or porous, as shown in Ref. [14]. The hollow

* Corresponding author. Tel.: +44 151 7944697; fax: +44 151 7944901.
E-mail addresses: taoxf@nim.ac.cn (X.F. Tao), y.y.zhao@liv.ac.uk (Y.Y. Zhao).
[1] Present address: National Institute of Metrology, Bei San Huan Dong Lu, Chaoyang District, Beijing 100013, PR China.

0921-5093/$ – see front matter © 2012 Elsevier B.V. All rights reserved.
http://dx.doi.org/10.1016/j.msea.2012.04.047

Table 1
Summary of structural and mechanical properties of the syntactic foams.

Syntactic foam	A	B	C	D
Microsphere volume, %	~60	~60	~60	~60
Microsphere size, μm	20–75	75–125	125–250	250–500
Hollow microspheres, %	98.2	90.5	32.2	2.0
Tensile strength, MPa	15.2	15.8	19.0	18.2
Shear strength, MPa	15.4	14.6	14.2	14.6
Compressive strength, MPa				
Confined	146	98	46	43
Unconfined	128.8	123.7	73.0	54.0
Plateau strength, MPa				
Confined	181.7	173.8	107.3	91.0
Unconfined	110.2	86.4	70.0	71.2

microspheres are nearly perfect spheres with a solid shell and a smooth surface. The porous microspheres are roundish with a relatively rough surface. Their inner structure is sponge like, normally containing a few big pores and numerous small pores. Both the hollow and porous microspheres have a similar porosity of about 80% and a similar effective particle density of 0.6 g/cm^3.

The as-received ceramic microsphere powder was divided into four size groups with the diameter ranges of 20–75, 75–125, 125–250 and 250–500 μm, which are designated as powders I, II, III and IV, respectively. By examining 1000 microspheres in the optical micrographs of the polished cross sections of the Al alloy syntactic foam samples manufactured from each of these powders, the percentages of hollow microspheres in powders I, II, III and IV were determined to be 98.2%, 90.5%, 32.2% and 2.0%, respectively.

Four types of Al alloy syntactic foam samples were fabricated by melt infiltration. They are designated as foams A, B, C and D, corresponding to the powders used: I, II, III and IV, respectively. The fabrication process was described in [12]. All the syntactic foams consisted of around 60% of ceramic microspheres and 40% of Al 6082 alloy by volume. The densities of the syntactic foam samples varied slightly in a narrow range of 1.40–1.45 g/cm^3. The standard T6 heat treatment [25] was performed on the as-fabricated samples. Specifically, the samples were homogenized in air at 540 °C for 100 min and then quenched in water, followed by ageing at 180 °C for 10 h.

Tensile, shear, confined compression and unconfined compression tests were performed on an Instron 4505 test machine. The cross-head speed for compression was 1 mm/min. A lower cross-head speed, 0.1 mm/min, was used for tension and shear because of the small fracture strains. For each type of Al alloy syntactic foam, at least three samples were tested to verify the reproducibility. The fracture surfaces of the samples after tensile tests were observed using a Hitachi scanning electron microscope. The cross sections of the samples after unconfined compression tests were observed using a Nikon optical microscope.

Fig. 1 shows the schematic diagrams of the setup for the tensile and shear tests. The tensile tests were performed on cuboidal samples with an approximate size of 38 × 12 × 5 mm. In each test, the sample was glued to two steel shims at each end to ensure a satisfactory test length. Before the steel shims were clamped to the test machine, two steel blocks with the same cross-section as the sample were inserted between the two steel shims at the two ends. The shear tests were performed on cylindrical samples with a diameter of 19 mm and a length of 24 mm. The test fixture was composed of two coupling halves of a steel cylinder. A 19-mm-diameter hole was drilled at the middle of the cylinder through the two halves in the transverse direction. The sample was placed in the hole such that it underwent a pure shear equal to the tensile load applied on the fixture. The location of the sample was adjusted by two screws at the two ends to ensure that the shearing took place at the middle of the sample. The uniaxial quasi-static confined and unconfined compression tests were carried out on cylindrical samples of a length about 24 mm and a diameter of 19 mm for the confined tests and 21 mm for the unconfined tests. In each confined test, the sample was contained within a cylindrical steel tube with its inner diameter equal to the sample diameter. The machine compliance for the compression tests was determined using a standard stiff sample and its effect was removed in calculating the strains.

3. Results and discussion

3.1. Tensile and shear strengths

The mean tensile and shear strength values of syntactic foams A, B, C and D are shown in Table 1. Syntactic foams A and B have slightly higher tensile strength values than syntactic foams C and D. All four syntactic foams have similar shear strength values.

Fig. 2 shows the micrographs of the typical tensile fracture surfaces for syntactic foams A, B, C and D. All the samples fractured in a brittle manner with very little plastic deformation and the fracture surface was perpendicular to the loading direction. Syntactic foams A and B have very flat fracture surfaces with most ceramic microspheres splitting apart, indicating crack propagation by cleavage. Syntactic foams C and D have less flat fracture surfaces with both trans-particle and inter-particle fracture present.

The tensile and shear tests showed that the syntactic foams are brittle and the tensile and shear strengths are insensitive to the type of the ceramic microspheres. The brittleness and the low tensile and shear strengths are an inherent weakness of the syntactic foams due to their unique structure. In these syntactic foams, the ceramic microspheres are densely packed and held together by a network of the Al alloy matrix. The bonding between the microspheres and

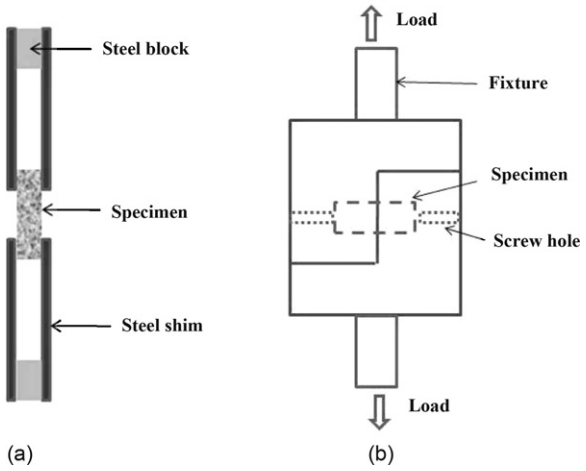

Fig. 1. Schematic diagrams of setup for (a) tensile and (b) shear tests.

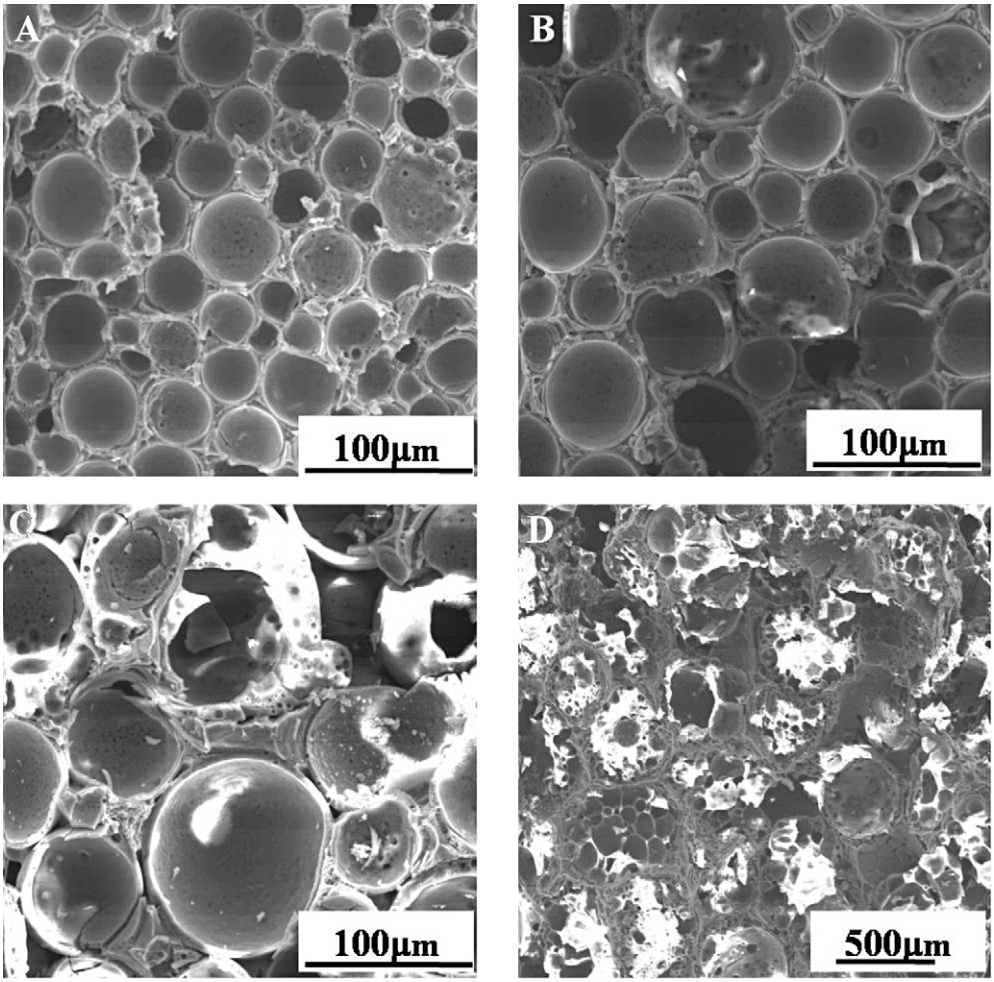

Fig. 2. SEM micrographs of the tensile fracture surfaces of syntactic foams A, B, C and D.

the Al alloy matrix is mechanical and not very strong. The tensile or shear load is largely borne by the metal matrix. The high volume percentage of the densely packed ceramic microspheres restricts the plastic deformation of the Al alloy matrix, resulting in the very low strains before fracture. The contacts between the adjacent microspheres are effectively cracks, which provide numerous sites for the initiation of fracture under stress concentration, leading to brittle failure at low stresses.

3.2. Confined compression response

Fig. 3 shows the representative engineering stress–strain curves of syntactic foams A, B, C and D under confined compression. All the curves have an initial linear region with steep increase in stress at low strains, followed by a plateau region where the strain increases rapidly with moderate increase in stress. In the linear region, the strain is composed of elastic deformation and a small amount of plastic deformation due to the closure of pores in the metal matrix. In the plateau region, the ceramic microspheres collapse or break up progressively with increasing stress, leading to a large increase in strain. For syntactic foams C and D, there is a clear boundary between the two regions, indicating that the ceramic microspheres start to collapse at a fixed stress. For syntactic foams A and B, the stress increases monotonically with strain and there is a gradual transition from the linear to the plateau region. Few stress drops are present during the transition, indicating occurrences of cracking and sudden deformation in the transverse or radial direction. However, these stress drops are small. This is because any transverse deformation was limited by the constraining tube jacket and the samples could only deform progressively along the axial direction.

The compressive response of the syntactic foams can be quantified by compressive and plateau strengths for comparison purposes. The compressive strength was taken as the maximum

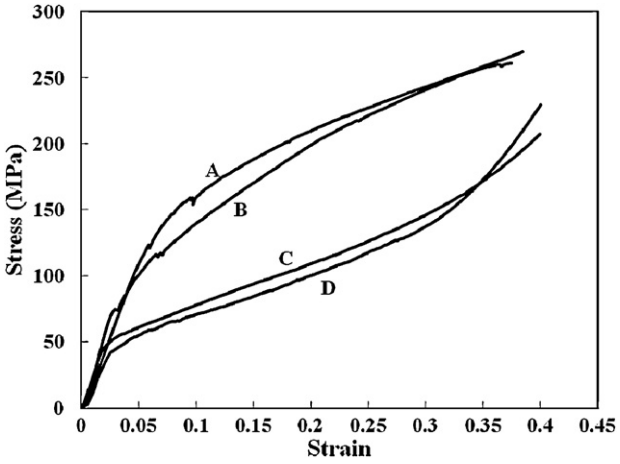

Fig. 3. Confined compressive engineering stress–strain curves of syntactic foams A, B, C and D.

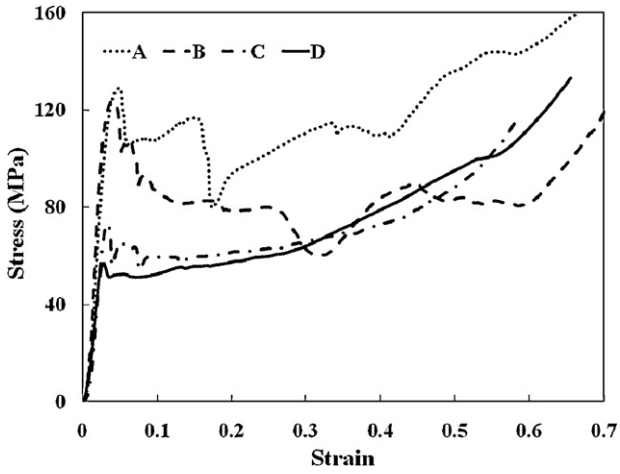

Fig. 4. Unconfined compressive engineering stress–strain curves of syntactic foams A, B, C and D.

stress of the linear region, or the stress at the intersection between the asymptotes of the linear and plateau regions when the transition between the two regions is gradual. In confined compression, the intermittent small stress drops due to cracking were ignored in determining the compressive strength, because the fracture of a sample does not affect its ability to support the compressive load. Therefore, the compressive strength in confined compression signifies the stress at which large-scale progressive collapse of the ceramic microspheres starts. The plateau strength was determined using the energy efficiency method, developed by Avalle et al. [26] and modified by Li et al. [27], but with a strain limit of 0.35 to facilitate comparison between the four syntactic foams.

The mean compressive and plateau strength values of syntactic foams A, B, C and D in confined compression are listed in Table 1. Although these syntactic foams contain a similar volume fraction of microspheres and the four types of microspheres have a similar density, syntactic foams A and B have considerably higher compressive and plateau strengths than syntactic foams C and D. The marked difference was due to the different structural characteristics of the microspheres. The majority of the ceramic microspheres in syntactic foams A and B (powders I and II) have a hollow structure, whilst those in syntactic foams C and D (powders III and IV) are mainly porous. Moreover, powders I and II have considerably smaller particles than powders III and IV. For the same density or porosity, hollow particles have a much higher strength than porous ones, and the particle strength generally decreases with particle size. Overall, powders I and II are much stronger than powders III and IV, resulting in stronger syntactic foams.

3.3. Unconfined compression response

Fig. 4 shows the representative engineering stress–strain curves for syntactic foams A, B, C and D under unconfined compression. Each curve has an initial linear region followed by a distinctive drop in stress. The four syntactic foams show different characteristics in the subsequent plastic deformation. Syntactic foams A and B have several random occurrences of large and sharp stress drops, for example, at a strain of about 0.15 for syntactic foam A and 0.25 for B. Syntactic foam C has a few small stress drops in the early stage of the plateau region, whilst syntactic foam D shows a smooth and relatively flat plateau region.

Fig. 5 shows the macrographs of the longitudinal cross sections of the representative samples of the four syntactic foams, compressed vertically to a strain of 0.2. In syntactic foams A and B, there are two pairs of major cracks. One pair develops from the top corners and another pair develops from near the bottom corners. They are inclined at an angle of about 30° to the loading direction and meet at a distance about one third from the top of the sample. A narrow, horizontal layer of crushed microspheres can be observed at the meeting location. Examining all the samples of syntactic foams A and B showed that the angle of the cracks to the loading direction was $31.6 \pm 2.2^\circ$. In syntactic foams C and D, the deformation is dominantly plastic with a broader crushed region. However, many small cracks are present in syntactic foam C, accompanied by radial expansion in the top two thirds of the sample. No visible shear crevasses or cracks are displayed on syntactic foam D, but barrelling is observed with radial expansion in the middle part of the sample. These observations indicate that the stress drops in the stress–strain curves in Fig. 4 were clearly caused by the formation of cracks.

The mean compressive and plateau strength values of syntactic foams A, B, C and D in unconfined compression are also listed in Table 1. The plateau strengths of syntactic foams A and B are much lower than their compressive strengths, due to stress drops in the plateau region. In contrast, the plateau strengths of syntactic foams C and D are similar to or higher than their compressive strengths, because they have a stable plateau region characteristic of progressive collapse of ceramic microspheres.

3.4. Failure mechanisms in unconfined compression

Figs. 4 and 5 show that the dominant failure mechanism in the syntactic foams was either plastic collapse or brittle fracture plus plastic collapse. Syntactic foams with weak ceramic microspheres (C and D) tend to fail by gradual collapse where the microspheres crumble under the compressive stress. Syntactic foams with strong ceramic microspheres (A and B) often fail by brittle fracture.

Plastic collapse occurs when the compressive stress exerted on the microspheres exceeds their compressive strength. The load partition between the metal matrix and the ceramic microspheres depends on the relative magnitudes of their elastic modulus, with the stiffer phase bearing a higher stress [28]. A study [9] on an Al matrix syntactic foam under uniaxial compression showed that the ceramic microspheres bear significantly more stress than the matrix by a factor of two.

The fracture failure of syntactic foams A and B has the characteristics of Griffith rupture for brittle solids subjected to uniaxial compression. In Griffith rupture, tensile stress concentration at the tips of one or more cracks induces fracture. Griffith rupture has two characteristic features: the fracture cracks propagate at a preferred angle of 30° to the loading direction; the compressive strength is eight times of its tensile strength [29,30]. Syntactic foams manufactured by melt infiltration are in effect aggregates of ceramic particles with the interstices filled with a metal network. The numerous contacts between the ceramic particles are effectively cracks, providing a favourable condition for Griffith rupture. In the present work, the cracks developed in syntactic foams A and B are inclined at an angle of $31.6 \pm 2.2^\circ$ to the loading direction, which is very close to the theoretical angle. The ratios of the compressive strength to the tensile strength for syntactic foams A and B are 8.5 and 7.8, respectively, which are also close to the theoretical ratio.

The orientations of the cracks developed in syntactic foams A and B deviated significantly from 45°, which is characteristic of shear fracture. This suggests that Griffith rupture had precedence over shear fracture in these foams, although they have very low shear strengths. A reasonable explanation is that the interlocking ceramic microspheres provide a high friction force against sliding between the surfaces of any cracks and therefore suppress the development of shear fracture in the syntactic foams.

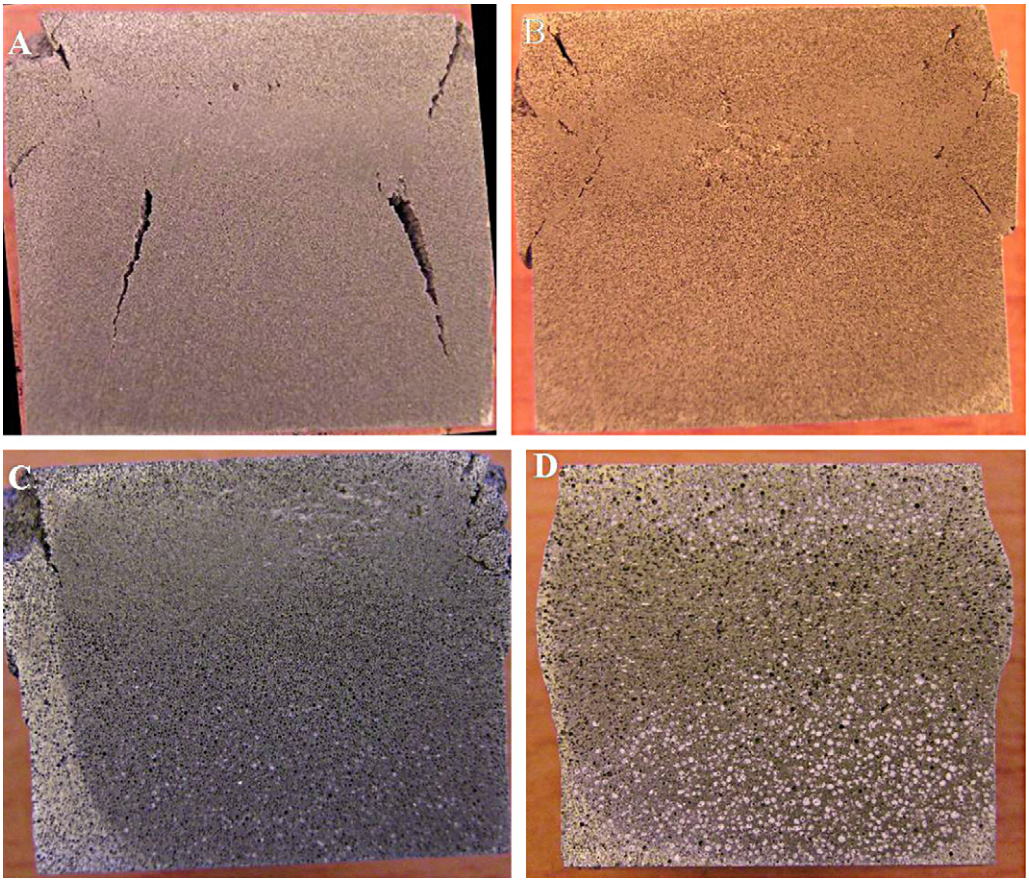

Fig. 5. Macrographs of longitudinal cross sections of syntactic foams A, B, C, and D, compressed to a strain of 0.2.

4. Conclusions

The four syntactic foams have similar tensile and shear strengths in the ranges of 15–19 and 14–16 MPa, respectively. In confined compression, all syntactic foams failed by the progressive collapse of the ceramic microspheres. In unconfined compression, syntactic foams A and B failed by brittle Griffith rupture. The major cracks were inclined at an angle of $31.6 \pm 2.2^{\circ}$ to the loading direction. The compressive strengths were in the range of 120–130 MPa. Syntactic foams C and D failed by progressive collapse of the ceramic microspheres. They have lower compressive strengths in the range of 50–75 MPa. The different compressive behaviour is mainly due to the different strengths of the ceramic microspheres. Stronger ceramic microspheres in syntactic foams A and B favour brittle fracture and weaker ceramic microspheres in syntactic foams C and D favour plastic collapse.

References

[1] S.P. Rawal, B.R. Lanning, in: M.S. Misra, A. Miravete (Eds.), Metal matrix composites, Proc. 9th Int. Conf. on Composite Materials, Madrid, 1993, pp. 203–210.
[2] P.K. Rohatgi, R.Q. Guo, H. Iksan, E.J. Borchelt, R. Asthana, Mater. Sci. Eng. A 244 (1998) 22–30.
[3] M. Hartmann, K. Reindel, R.F. Singer, Mater. Res. Soc. Symp. Proc. 521 (1998) 211–216.
[4] J. Banhart, M.F. Ashby, N.A. Fleck, Metal Foams and Porous Metal Structures, Verlag MIT Publishing, Bremen, 1999.
[5] M. Kiser, M.Y. He, F.W. Zok, Acta Mater. 47 (1999) 2685–2694.
[6] D.K. Balch, D.C. Dunand, A. Ghosh, T. Sanders, D. Claar (Eds.), Processing and Properties of Lightweight Cellular Metals and Structures, TMS, Warrendale, 2002, pp. 251–260.
[7] A.H. Brothers, D.C. Dunand, Appl. Phys. Lett. 84 (2004) 1108–1110.
[8] D.K. Balch, J.G. O'Dwyer, G.R. Davis, C.M. Cady, G.T. Gray III, D.C. Dunand, Mater. Sci. Eng. A 391 (2005) 408–417.
[9] D.K. Balch, D.C. Dunand, Acta Mater. 54 (2006) 1501–1511.
[10] P.K. Rohatgi, J.K. Kim, N. Gupta, S. Alaraj, A. Daoud, Composites A 37 (2006) 430–437.
[11] G.H. Wu, Z.Y. Dou, D.L. Sun, L.T. Jiang, B.S. Ding, B.F. He, Scr. Mater. 56 (2007) 221–224.
[12] L.P. Zhang, Y.Y. Zhao, J. Compos. Mater. 41 (2007) 2105–2117.
[13] A. Daoud, Mater. Sci. Eng. A 488 (2008) 281–295.
[14] X.F. Tao, G.K. Schleyer, Y.Y. Zhao, IUTAM Bookseries, vol. 12, 2009, pp. 97–104.
[15] X.F. Tao, L.P. Zhang, Y.Y. Zhao, Mater. Des. 30 (2009) 2732–2736.
[16] Q. Zhang, P.D. Lee, R. Singh, G. Wu, T.C. Lindley, Acta Mater. 57 (2009) 3003–3011.
[17] X.F. Tao, Y.Y. Zhao, Scr. Mater. 61 (2009) 461–464.
[18] I.N. Orbulov, J. Dobránszky, Á. Németh, J. Mater. Sci. 44 (2009) 4013–4019.
[19] I.N. Orbulov, Á. Németh, J. Dobránszky, J. Phys. Conf. Ser. 240 (2010) 012168.
[20] I.N. Orbulov, J. Ginsztler, Composites A 43 (2012) 553–561.
[21] L.J. Gibson, M.F. Ashby, Cellular Solids: Structure and Properties, second ed., Cambridge University Press, Cambridge, 1997.
[22] N. Gupta, Kishore, E. Woldsenbet, S. Sankaran, J. Mater. Sci. 36 (2001) 4485–4491.
[23] N. Gupta, E. Woldesenbet, J. Mater. Sci. 37 (2002) 3199–3209.
[24] N. Gupta, E. Woldesenbet, P. Mensah, Composites A 35 (2004) 103–111.
[25] ASM Handbook Committee, Heat Treating of Alluminum Alloys, ASM, Handbook, vol. 4, ASM International, Materials Park, 1991, pp. 841–879.
[26] M. Avalle, G. Belingardi, R. Montanini, Int. J. Impact Eng. 25 (2001) 455–472.
[27] Q.M. Li, I. Magkiriadis, J.J. Harrigan, J. Cell Plast. 42 (2006) 371–392.
[28] D. Hull, T.W. Clyne, An Introduction to Composite Materials, Cambridge University Press, Cambridge, 1996.
[29] A.A. Griffith (Ed.), Proc. First Int. Cong. Applied Mechanics, Delft, 1924, pp. 55–63.
[30] D.S. Jayatilaka, Fracture of Engineering Brittle Materials, Applied Science Publishers, London, 1979.